

Optimizing the efficiency of femtosecond-laser-written holograms

K. J. Wædegaard · H. D. Hansen · P. Balling

Published online: 23 May 2013
© Springer-Verlag Berlin Heidelberg 2013

Abstract Computer-generated binary holograms are written on a polished copper surface using single 800-nm, 120-fs pulses from a 1-kHz-repetition-rate laser system. The hologram efficiency (i.e. the power in the holographic reconstructed image relative to the incoming laser power) is investigated for different laser-structuring parameters. Theoretical diffraction grating efficiencies for a binary amplitude grating show good agreement with the experimental measurements for diameters of the laser-formed holes below the pitch. Modelling based on straightforward geometrical arguments is used to find the optimal hole size. For a coverage (i.e. relative laser-structured area) of $\sim 43\%$, the efficiency reaches $\sim 10\%$, which corresponds to a relative power transferred to one reconstructed image of $\sim 20\%$. The efficiency as a function of pitch (for fixed coverage) is fairly constant from 2 to 6 μm .

1 Introduction

Computer-generated holograms (CGHs) are holographic interference patterns that are calculated numerically—as opposed to a classical hologram, which is a photography-like recording of an actual optical interference pattern. CGHs were first demonstrated in 1967 by Lohmann and Paris [1], and several different computational techniques have been demonstrated [2, 3]. The feasibility of writing CGHs directly by ultrashort laser pulses has been demonstrated previously, for example, on silicon surfaces [4], inside glasses [5] and by evaporation of metal films on

glass substrates [6]. The ultrashort laser pulse duration provides a high writing resolution due to minimized heat-propagation effects [7, 8]. In addition, the technique is highly versatile, since the method can be applied on all flat, reflecting materials. Laser-written CGHs have various potential applications such as security marking, anti-counterfeiting, beam shaping [9] and holographic data storage [10], in specific cases even with the possibility of erasing and rewriting [11]. Naturally, the hologram efficiency (i.e. the ability to transfer power to the holographic reconstruction) is important to all applications. We present a systematic investigation of changes in the hologram properties when the geometry of the laser-written areas is controlled. Optimal hologram parameters are determined.

2 Experiment

Holograms are written on polished copper surfaces using 800 nm, 120 fs laser pulses from a 1-kHz-repetition-rate laser system. The beam is focused onto the sample surface using an aspheric lens with a focal length of 10 mm and $\text{NA} = 0.545$. The size of the ablated holes is controlled by adjusting the pulse energy, which is in the range 0.2–7 μJ . The actual size of the holes is determined using scanning electron microscopy (SEM). A gentle flow of helium is applied through a nozzle enclosing the focusing beam to prevent breakdown in the air and remove laser-generated debris. The sample reflectivity is significantly reduced in the laser-structured areas. For the present work, copper was selected because it has a high reflectivity and it is relatively inexpensive, but the CGHs can be written on any reflecting surface.

The sample motion is done by computer-controlled stages. The writing speed has increased significantly

K. J. Wædegaard · H. D. Hansen · P. Balling (✉)
Department of Physics and Astronomy,
Aarhus University, DK-8000 Aarhus C, Denmark
e-mail: balling@phys.au.dk

compared to Ref. [4] by applying in one direction a fast, precise, magnetically driven air-bearing stage. Using the position-sensitive output from the stage controller, the individual pixels of the CGH can be written by a single laser pulse during the stage motion. The positional accuracy is better than one micrometre. Typical holograms of $2 \times 2 \text{ mm}^2$ are written in $\sim 10 \text{ min}$.

The CGHs are calculated as binary Fresnel holograms as in Ref. [4]. The hologram is divided into a finite grid of square pixels that are placed side by side. The pitch is the distance between the centres of neighbouring pixels. Hence, the area of one pixel is the square of the pitch. For each pixel, the real part of the complex electric field of the object is calculated. The binary bit pattern is generated by setting all pixels in the grid with values below the median level to 0 and the rest to 1. The actual hologram is generated by transferring the calculated bit pattern to the sample by selective ablation, such that half the pixels are absorbing and half are reflecting. No pre- or post-treatment of the sample is necessary. The holographic images are reconstructed on a white screen using a 2-mW He–Ne laser at 633 nm. A digital camera is used to record images of the screen for quantitative measurements of the hologram efficiency.

3 Results and discussion

An example of an image reconstructed from a laser-written hologram is shown in Fig. 1. The image shows both the normal and the inverted reconstructed image of the first diffraction order on each side of the 0th order spot. If the hologram efficiency is characterized by the power in one holographic reconstruction (i.e. the top right pattern in Fig. 1) relative to the power of the incident beam, this efficiency can be measured as a function of the hologram parameters.

The efficiency of a one-dimensional binary amplitude grating can be determined theoretically. The normalized amplitude of the m th diffraction order is given by [12]

$$G_m = \exp(-im\pi) \int_0^{m2\pi} \frac{1}{m2\pi} \exp(i\Theta) d\Theta, \quad (1)$$

where a is the fill factor (i.e. the ratio of the reflecting to the total area of the grating). The efficiency of the diffraction order is then given by

$$\eta_m = |G_m|^2 = \frac{\sin^2(ma\pi)}{m^2\pi^2}. \quad (2)$$

For the first diffraction order, the maximum diffraction efficiency is found for a fill factor of $a = \frac{1}{2}$ to be $\frac{1}{\pi^2}$ (i.e.

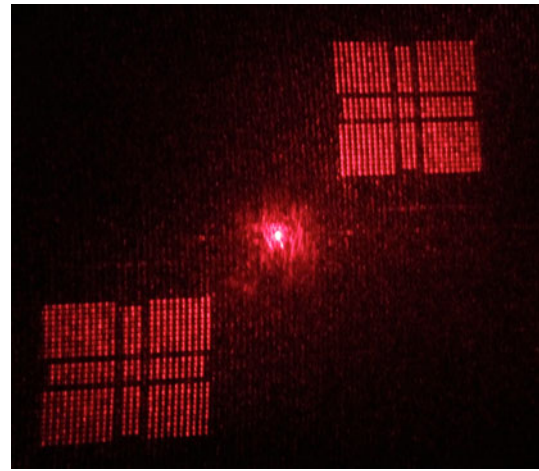


Fig. 1 Example of a reconstructed holographic image used to characterize the efficiency. Here, the efficiency is defined as the ratio of the power in one reconstructed image (i.e. the *top right* pattern) to that of the incident beam

10.1 %). Note that this efficiency is actually higher than for a sinusoidal amplitude grating, where the maximum efficiency of the first diffraction order is only 6.25 % [2, 13]. However, the sinusoidal diffraction grating has the advantage of suppressing higher-order diffraction peaks.

Figure 2 shows the efficiency as defined above versus the diameter of individual laser holes for a fixed pitch of $6 \mu\text{m}$. The coverage (i.e. relative area covered by ablated pixels), $A(d)$, for a given diameter, d , is determined by geometrical calculations based on the actual pixel positions and the circularity of the holes for each individual CGH. For diameters $< 6 \mu\text{m}$, the covered area is simply given by the area of all the holes and is therefore proportional to the diameter squared. However, above $6 \mu\text{m}$ the ablated regions start to overlap; hence, the covered area is less than the sum of the individual areas. The partly full ($d \leq 6 \mu\text{m}$), partly dashed ($d > 6 \mu\text{m}$) line is the theoretical efficiency given by Eq. 2, with a fill factor of $a(d) = 1 - A(d)$. For diameters up to and a bit above the pitch, the theory reproduces the experimental measurements well without any scaling of the experimental data. However, at larger diameters (i.e. smaller fill factor) the theory overestimates the efficiency. This is probably due to the fact that the theory is based on a regular periodic grating. The irregularity of the hologram causes the above-mentioned overlapping of pixels to be more random, which decreases the holographic reconstruction efficiency compared to that of a perfect periodic grating.

To determine the diameter and coverage, where the efficiency is the highest, the experimental data are fitted to a simple model. It is assumed that the efficiency increases linearly with the coverage until a maximum is reached and

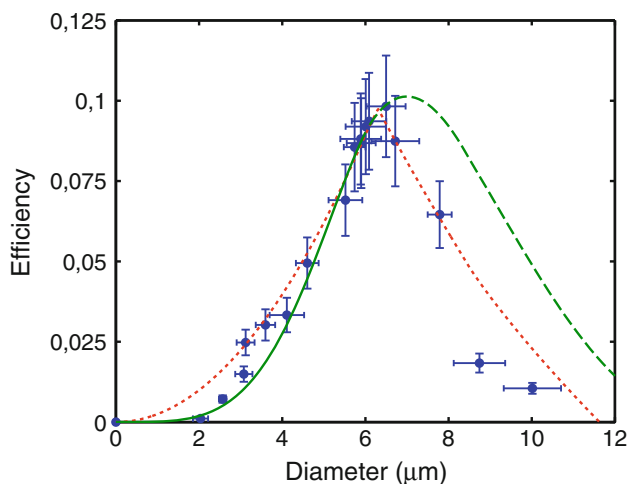


Fig. 2 Measured efficiency (data points) of the holographic reconstruction as a function of the hole size, together with the theoretical diffraction grating efficiency (full and dashed line), and a fit (dotted line) to a model described in detail in the text. The horizontal error bars represent the statistical spread of the measured diameters. The vertical error bars represent an estimate of the efficiency uncertainty determined from the holographic images

then decreases linearly with the same slope. That is, the efficiency is fitted with the piecewise function given by

$$\eta(d) = \begin{cases} cA(d) & \text{for } d \leq d_{\text{opt}} \\ c[2A(d_{\text{opt}}) - A(d)] & \text{for } d > d_{\text{opt}} \end{cases}, \quad (3)$$

where the slope, c , and the optimal diameter, d_{opt} , are free parameters in the fit. The dotted line in Fig. 2 shows the fit to this model. The fit does not reproduce the initial evolution of the efficiency as well as the analytic theory, but it reproduces the sharp bend and the following rapid decrease more accurately. The optimal diameter is found from the fit to be $6.3 \pm 0.2 \mu\text{m}$. Combined with exactly half the pixels being ablated, this corresponds to an optimal coverage of $A(d_{\text{opt}}) = 43 \pm 2\%$. The CGHs are calculated as being made up of square pixels, but in reality, the ablated regions are circular. If the hole diameter is equal to the pitch, the ablated region only covers part of the intended pixel area so that $A(d = \text{pitch}) = 39\%$. On the other hand, if the ablated area for a single hole is set to be equal to the area of the square pixel, the diameter has to be $2/\sqrt{\pi} (\simeq 1.13)$ times larger than the pitch, which gives $A(d) = 48\%$. However, as mentioned above, when the hole diameter exceeds the pitch, adjacent holes start to overlap and parts of pixels that were supposed to be reflecting become absorbing. Therefore, the optimal diameter and coverage is a compromise between the two. The theoretical optimal coverage is 50%, which is reached at a pitch of about $7 \mu\text{m}$, but at this coverage, the overlap is too dominant and the efficiency has dropped significantly. Nevertheless, the maximum efficiency achieved in the experiment is $\sim 10\%$, which is

close to the theoretical maximum of 10.17%. The maximum efficiency achieved for these reflection holograms compares with that achieved for volume gratings also produced by femtosecond lasers, where a maximum efficiency of $\sim 15\%$ is reached [14]. The theoretical maximum for binary volume holograms is 4 times higher (i.e. 40.5%) than for thin holograms [15].

The efficiency, which is directly proportional to the absolute power in the reconstruction, may not be the most appropriate measure for the quality of the reconstruction. Therefore, we define the transferred power ratio (TPR) as the power in one reconstruction relative to the sum of the powers in the 0th order spot and the two first-order reconstructions. This gives a relative measure of how much power is transferred from the directly reflected beam into the holographic reconstruction and thereby how clearly the reconstructed image appears relative to the central (0th order) spot.

Figure 3 shows the TPR as a function of diameter for the same data shown in Fig. 2. The theoretical TPR (full and dashed line) has again been calculated by Eq. 2 (note: the 0th-order diffraction efficiency is simply given by $E_0 = a^2$). Again, the theory reproduces the experimental data well up to and a bit above the pitch, and not very well at larger diameters. The theory actually predicts a continuously increasing TPR that approaches $\frac{1}{3}$ (or 33%) for the coverage approaching 100%. Nevertheless, for the same reasons as mentioned above, the measured TPR in fact reaches a maximum value for an optimal diameter and coverage.

Once again, a simpler model has been used to fit the data to determine the optimal values. There is a decrease in the

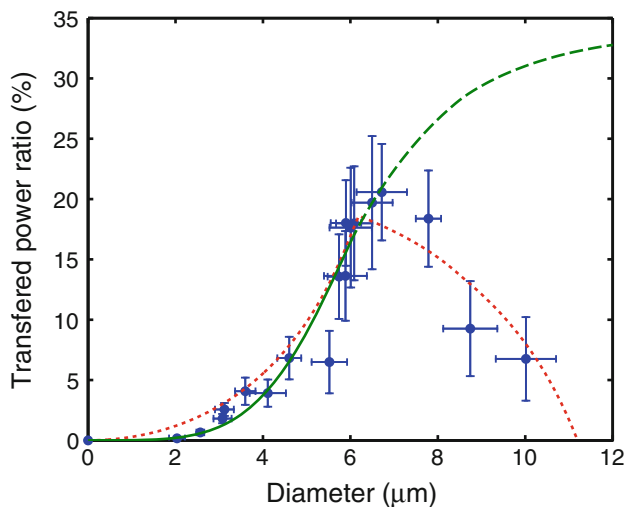


Fig. 3 Measured TPR (data points) of the holographic reconstruction as a function of the hole size, together with the theoretical calculations (full and dashed line), and a fit (dotted line) to a model described in detail in the text

total power reflected from the hologram with increasing diameter, due to the corresponding decrease in the area of the reflecting part of the hologram. Measurements show that the total power drops linearly with the reflecting area (data not shown), as expected by summation of Eq. 2 over all diffraction orders. Hence, the data in Fig. 3 are fitted to Eq. 3 divided by a function that is linearly decreasing with $A(d)$:

$$\text{TPR}(d) = \begin{cases} \frac{cA(d)}{1-A(d)} & \text{for } d \leq d_{\text{opt}} \\ \frac{c[2A(d_{\text{opt}})-A(d)]}{1-A(d)} & \text{for } d > d_{\text{opt}} \end{cases}, \quad (4)$$

In this fit (dotted line in Fig. 3), the optimal diameter is found to be $6.2 \pm 0.2 \mu\text{m}$ corresponding to an optimal coverage of $42 \pm 2 \%$, which agrees within uncertainties with the fit in Fig. 2. About 20 % of the power (see Fig. 3) is transferred into the reconstructed image at hole diameters close to the optimal one, which fits well with the theoretical value of 22 % at a coverage of 50 %.

The reconstruction efficiency has also been tested as a function of the hologram pitch. For these measurements, CGHs have been calculated to reconstruct the same image (shown in Fig. 1), but with different pitches resulting in different CGH patterns. When increasing the resolution (i.e. decreasing the pitch) larger holographic images can be reconstructed without overlap between different diffraction orders [4]. In each calculation, the size of the reconstructed image is scaled to take up the same relative area between 0- and higher-order diffraction spots—this means that the actual size of the reconstructed image increases with decreasing pitch. In this experiment, when writing the CGHs on the copper sample, the diameter of the holes is kept almost the same as the pitch, which ensures that the

coverage is constant ($\sim 39 \%$). Fig. 4 shows the TPR as a function of the pitch. For pitches up to $6 \mu\text{m}$, the TPR is seen to be fairly constant. As expected, the power in a reconstructed image does not increase with increased resolution, since the maximum efficiency is already reached at the $6 \mu\text{m}$ pitch. However, although it does not increase the diffraction efficiency, the increased resolution has several advantages. First, as mentioned above, it enables reconstruction of larger images without overlap between different diffraction orders. Second, owing to the increase in information in the hologram, the increased resolution gives sharper images, which means that more detailed objects can be successfully reconstructed [4].

4 Conclusion

The efficiency of computer-generated holograms written directly on a surface by ultrashort laser pulses has been investigated as a function of the hologram parameters. Theoretical calculations of the diffraction efficiency and TPR for a one-dimensional binary amplitude grating reproduce the experimental data well for hole diameters up to the pitch. However, for diameters above the pitch, the ablated holes start to fill some of the pixels that should be reflecting, and thus the theory and experimental data disagree. By fitting to simple coverage-dependent models, a hole diameter of $\sim 6.2 \mu\text{m}$ corresponding to a coverage of $\sim 42 \%$ is found to optimize the hologram reconstruction efficiency. At this optimum, the TPR reaches $\sim 20 \%$ and the efficiency $\sim 10 \%$, which is in good agreement with the theoretical maximum of 10.1 %. Variations in the pitch for a fixed coverage showed that the TPR was fairly constant from 2 to $6 \mu\text{m}$.

Acknowledgments This work was supported by The Danish Council for Independent Research | Natural Sciences (FNU).

References

1. A.W. Lohmann, D.P. Paris, *Appl. Opt.* **6**, 1739 (1967)
2. P. Harihan, *Optical Holography, Principles, Techniques, and Applications*, 2nd ed. (Cambridge University Press, New York, 1996)
3. O. Bryngdahl, F. Wyrowski, in *Digital Holography—Computer-Generated Holograms in Progress in Optics* 28, ed. by E. Wolf (Elsevier, Amsterdam, 1990)
4. K.J. Wædegaard, P. Balling, *Opt. Express* **19**, 3434 (2011)
5. Y. Li, Y. Dou, R. An, H. Yang, Q. Gong, *Opt. Express* **13**, 2433 (2005)
6. Q.-Z. Zhao, J.-R. Qiu, X.-W. Jiang, E.-W. Dai, C.-H. Zhou, C.-S. Zhu, *Opt. Express* **13**, 2089 (2005)
7. D. Buerle, *Laser Processing and Chemistry*, 4th ed. (Springer, Berlin, 2011)
8. P. Balling, chapter 14 in *Laser Cleaning II*, ed. D. M. Kane (World Scientific Publishing, Singapore 2006)
9. Z. Guo, S. Qu, S. Liu, *Opt. Commun.* **273**, 286 (2007)

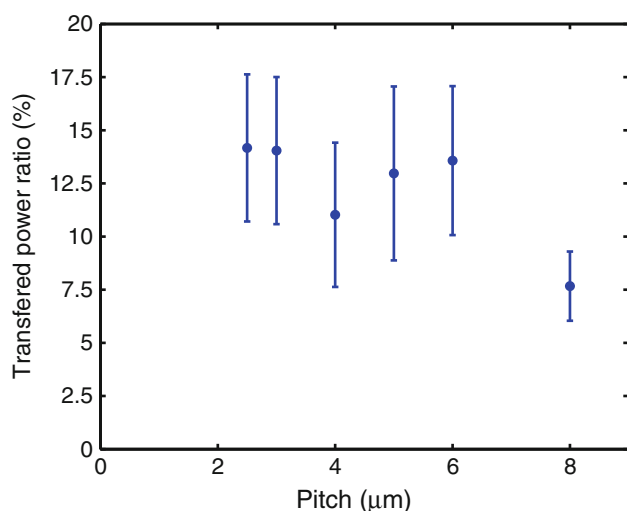


Fig. 4 Measured TPR as a function of hologram pitch for a fixed coverage of $\sim 39 \%$. The pitch uncertainty is less than the data point size

10. Y. Li, W. Watanabe, K. Itoh, X. Sun, *Appl. Phys. Lett.* **81**, 1952 (2002)
11. R.S. Taylor, C. Hnatovsky, E. Simova, P.P. Rajeev, D.M. Rayner, P.B. Corkurn, *Opt. Lett.* **32**, 2888 (2007)
12. A. Martínez, M.d.M. Sánchez-López, I. Moreno, *Eur. J. Phys.* **28**, 805 (2007)
13. G.K. Ackermann, J. Eichler, *Holography, A Practical Approach*. (Wiley-VCH Verlag GmbH, Weinheim, 2007)
14. K. Zhou, Z. Guo, W. Ding, S. Liu, *Opt. Express* **18**, 13640 (2010)
15. de T.M. Jong, de D.K.G. Boer, C.W.M. Bastiaansen, *Opt. Express* **19**, 15127 (2011)